

Fabrication of Electrochemical Sensor with Tunable Electrode Distance

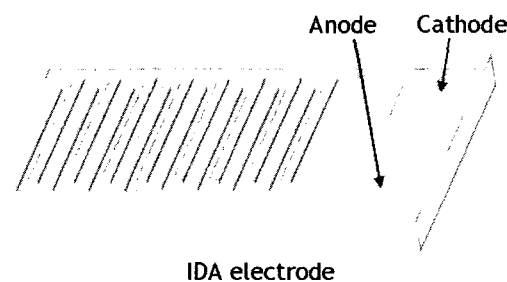
Yuheon Yi and Je-Kyun Park

Abstract—We present an air bridge type electrode system with tunable electrode distance for detecting electroactive biomolecules. It is known that the narrower gap between electrode fingers, the higher sensitivity in IDA (interdigitated array) electrode. In previous researches on IDA electrode, narrower patterning required much precise and expensive equipment as the gap goes down to nanometer scale. In this paper, an improved method is suggested to replace nano gap patterning with downsizing electrode distance and showed that the patterning can be replaced by thickness control using metal deposition methods, such as electroplating or metal sputtering. The air bridge type electrode was completed by the following procedures: gold patterning for lower electrode, copper electroplating, gold deposition for upper electrode, photoresist patterning for gold film support, and copper etching for space formation. The thickness of copper electroplating is the distance between upper and lower electrodes. Because the growth rate of electroplating is $0.5 \mu\text{m min}^{-1}$, the distance is tunable up to hundreds of nanometers. Completed electrodes on the same wafer had $5 \mu\text{m}$ electrode distance. The gaps between fingers are 10, 20, 30, and $40 \mu\text{m}$ and the widths of fingers are 10, 20, 30, 40, and $50 \mu\text{m}$. The air bridge type electrode system showed better sensitivity than planar electrode.

Index Terms—Three-dimensional electrode system, Tunable electrode distance, Electrochemical sensor, Copper electroplating

I. INTRODUCTION

Interdigitated array (IDA) electrodes have been studied as a mean to improve sensitivity on detecting electroactive species of which oxidized form is converted into reduced form and *vice versa*. The reaction takes place on gold or platinum surface under external electric potential. The IDA electrode has two pairs of working electrodes consisting of parallel metallic legs that are interdigitated and insulated [1]. Figure 1 shows the schematic diagram of conventional planar IDA electrode and the concept of redox recycling of electroactive species on an IDA electrode. Ferrocyanide is converted into ferricyanide when the applied potential is higher than 350 mV with respect to Ag/AgCl reference electrode. Ferricyanide is transformed into ferrocyanide when the external electric potential is lower than -50mV. In oxidation reaction, one



ex) Ferrocyanide-ferricyanide

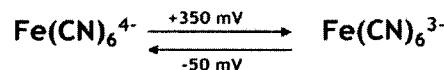


Fig. 1. Concept of conventional planar IDA electrode and redox recycling of electroactive species

electron comes from one ion of ferrocyanide and it enters one of the IDA electrodes, the anode. The loss of electron forms anodic current. Symmetrically one ion of ferricyanide extracts one electron from the cathode in reduction process. The gain of electron becomes cathodic current. Consequently, one ion of ferrocyanide experience repeated reduction and oxidation a lot of times according to the number of fingers of IDA electrodes. Additionally, narrow width of electrode and narrow gap between fingers raise the possibility of conversion exceedingly, and make the total detectable current so higher that the IDA electrodes have high sensitivity.

As described above, interdigitated array (IDA) electrode has been researched extensively [2-4] because it is one of the most effective structures for detecting electroactive species, such as ferrocyanide / ferricyanide couple and p-aminophenol / quinoneimine couple. The repeated reduction and oxidation reactions on each electrode band give higher Faraday current. It is also known that the narrower gap between electrode fingers results in the higher sensitivity [5, 6]. Therefore, patterning techniques are the only ways to enhance sensitivity in case of IDA electrodes. Hot embossing lithography has possibility as a novel technique for the replication of nanostructures. Replication fidelity in polymers of less than 10 nm was achieved using anisotropically etched silicon substrates as masters. It was demonstrated that nanoimprinting combined with the lift-off technique was used to fabricate the arrays of interdigitated metal electrodes. The electrodes had a length of 100 μm and a space between the electrodes of 200 nm [7].

As the gap goes down to nanometer scale, however, narrow patterns require much more precise and expensive equipment. In this paper, it is suggested that the nano-patterning can be replaced by thickness control. Structure of the IDA electrode has to be changed from planar to three dimensional one in order to realize thickness control. There are some approaches for three dimensional electrodes. One is comb IDA electrodes for more rapid and sensitive bead-based immunoassay proposed by Kim *et. al.* [1]. In their study, signal amplification was achieved through coupling the redox cycling of IDA electrodes with an enzyme label. Comb IDA electrodes enhanced the signal 3 times higher than planar IDA electrodes. Comb IDA electrodes enabled positioning the beads and attached

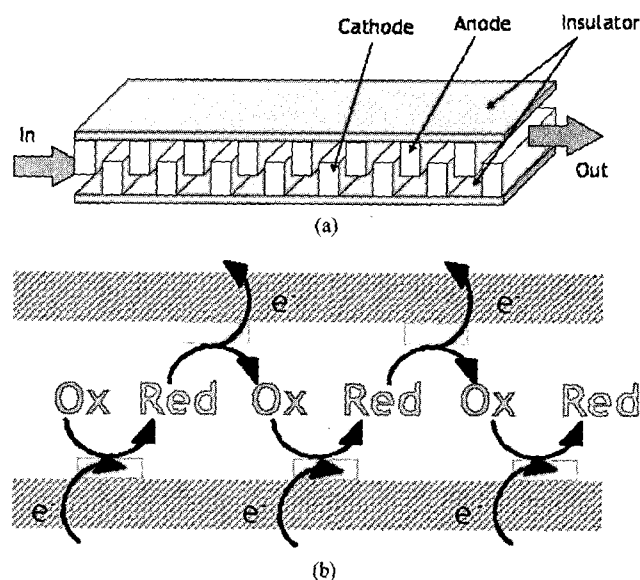


Fig. 2. (a) Conceptual view of the proposed 3-D electrode systems. (b) Redox recycling of electroactive species in 3-D electrodes. Upper electrodes are anode and lower are cathodes

enzyme closer to the sensing electrodes [1, 8]. Another research is 3-D comb electrodes for amperometric immunosensors published by Honda *et. al.* [9]. The fabrication was simple and the biosensor was efficient. The dimensions of the 3-D electrodes were 10-20 μm in width, 10-20 μm spacing and 20-30 μm in height. The 3-D comb electrodes are applicable for high sensitive enzyme immunoassays.

In this paper a new type of three dimensional electrode was proposed. Its name is air bridge type electrode. The name came from the shape of the electrode. There is air space between lower electrode and upper electrode. In this paper, the space is called as distance. Figure 2 shows the conceptual view of the proposed 3-D electrode systems. The detailed design and fabrication is mentioned in the following design and fabrication.

II. DESIGN AND FABRICATION

1. Electrode Design

Electrodes are located upper and lower plane and they are facing each other. Each electrode has 20 to 30 fingers according to the finger width and the finger gap. The electrodes are aligned to put one finger of lower electrode

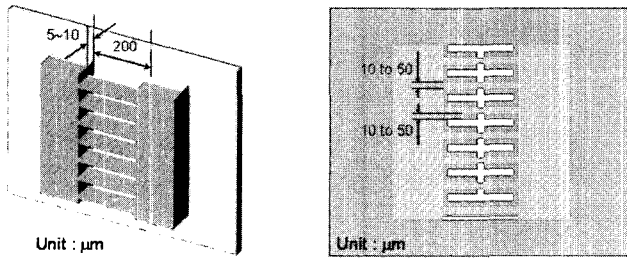


Fig. 3. Schematic of the air bridge type electrode and its dimensions

between two fingers of upper electrode. Therefore, the view from above shows the fingers of air bridge type electrodes are interdigitated in other planes. The upper electrode is anode and the lower is cathode and *vice versa* because they are symmetric. There is very tiny distance between electrodes. The most important point of the air bridge type electrodes is the controllability of the distance. The fabrication process will be stated in the following section. The distance is formed by removing sacrificial layer. The forming of the sacrificial layer is based on electroplating. The thickness of electroplated metal is determined by current density and growth time. Generally the growth rate is sub micrometer per minute, which means the thickness can be controlled up to hundreds of nanometers. The sensitivity of the air bridge type electrode will increase by reducing the distance between the electrodes.

There are three decisive factors of the air bridge type electrode. One is the finger width of electrode and the range is 10 μm to 50 μm . Another is the gap between fingers and the range is 10 μm to 50 μm . The third is the height of channel, that is, the distance between electrodes facing each other. The distance is 5 μm to 10 μm as shown in Figure 3.

2. Fabrication

Pyrex glass wafer of which thickness was 500 μm was prepared. By sputtering, 50 nm of chrome and 100 nm of gold were deposited successively. AZ1512 positive photoresist (PR) was spin-coated. The spin speed was 4000 rpm for 30 s. For 90 s, the wafer was soft-baked for dry surface in a 100 $^{\circ}\text{C}$ convection oven. It was exposed through the first mask to UV light with the energy of 100 mW cm^{-2} . The wafer was developed in AZ300MIF developer for 60 s. At last, the wafer was hard-baked for 2

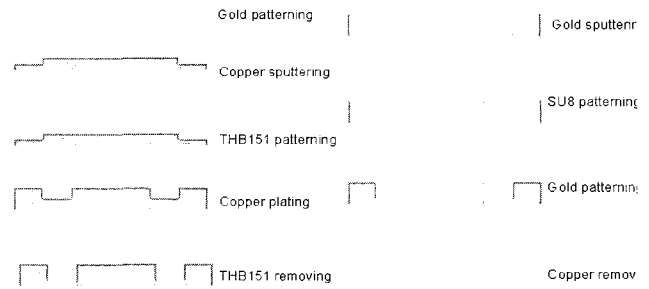


Fig. 4. Fabrication process of the air bridge type electrode

min in 120 $^{\circ}\text{C}$. Gold of the wafer was etched out by mixture of KI and I_2 solutions. Chrome was removed by chrome etchant, CR-7SK. The PR was oxidized in piranha solution (a 3:1 mixture of concentrated H_2SO_4 and 30 % H_2O_2) for 10 min. The first step was completed with a result of the gold patterned glass wafer.

The second began by copper sputtering for electroplating seed layer by 100 nm in thickness. On copper layer THB-151N negative PR made by JSR was spin-coated. The thickness was about 50 to 70 μm by varying spinning speed from 800 to 650 rpm. Air stabilization on flat plate for 30 min was needed to prevent possible reflow in a hot oven because the PR has not only high thickness but also relatively low viscosity. Soft bake was performed in a 120 $^{\circ}\text{C}$ oven for 30 min. The wafer was exposed to UV light of which dose 1000 mW cm^{-2} to 1500 mW cm^{-2} . Developer, THB-D2 was supplied by JSR. It took about 20 to 30 min under dipping development. The wafer was then copper electroplated up to 10 and 20 μm for sacrificial layer. The plating solution was Microfab Cu-300 supplied by EEJA. The other conditions were in Table 1. The PR was stripped for Cr/Au sputtering by JSR THB-S1 stripper. Proper temperature was 60 $^{\circ}\text{C}$ and time was 20 min. The sputtering condition was the same as the condition of preparing gold sputtered glass wafer.

SU-8 2025 negative PR coating was the beginning of the third step. The PR was spin-coated. The spin speed was

Table 1. Copper electroplating condition [10]

| | |
|------------------|--|
| Plating solution | EEJA MicroFab Cu-300 |
| Copper ingot | Containing phosphorus 3 % |
| Current density | 30-40 mA cm^{-2} |
| Temperature | Room temperature |
| Power supply | Agilent E3646A |
| Extraction rate | Approximately 0.5 $\mu\text{m min}^{-1}$ |

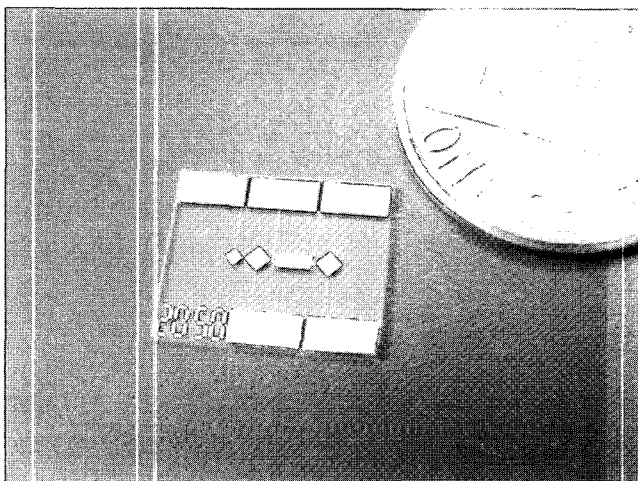
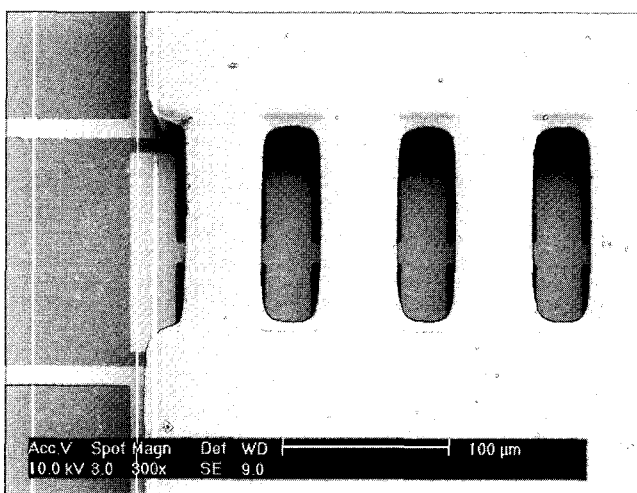
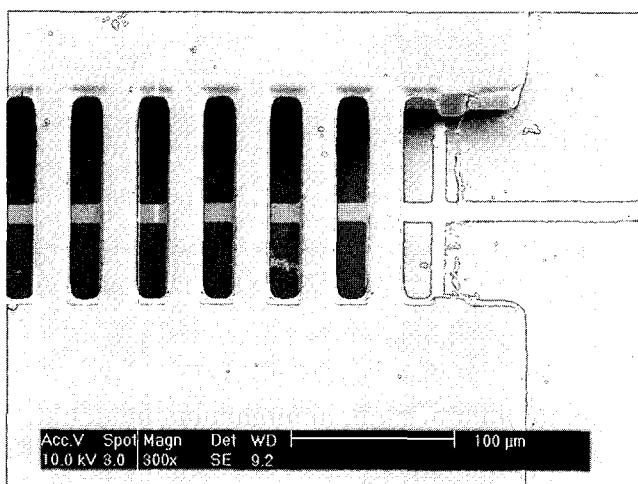


Fig. 5. Overall device having 20 μm finger width and 50 μm finger gap



(a)



(b)

Fig. 6. SEM image of the air bridge type electrode. (a) Finger gap is 50 μm and finger width is 40 μm . (b) Electrode has 20 μm finger gap and 20 μm finger width

2500 rpm for 30 s for about 20 to 30 μm thickness. For 5 min, the wafer was soft-baked for dry surface in a 95 $^{\circ}\text{C}$ convection oven. It was exposed through the first mask to UV light with the energy of 300 mW cm^{-2} . SU-8 required post exposure bake for 3 min in a 95 $^{\circ}\text{C}$ convection oven. The wafer was developed in SU-8 developer for 5 min. Hard bake was not required. The SU-8 patterned wafer was soaked in gold etchant and chrome etchant consecutively until the copper sacrificial layer was disappeared. Washing the wafer with isopropyl alcohol was the last process for anti-stiction. Figure 4 shows the whole processes. Figure 5 and 6 are an overall device and SEM images of two different electrodes having 20 μm finger gap and width and 50 μm finger gap and 40 μm finger width. The distance between upper electrode and lower electrode is about 5 μm .

III. EXPERIMENTAL

1. Preparation for Electrochemical Experiment

Before measuring electrochemical characteristics, it is useful to dissolve potassium ferrocyanide in phosphate buffer solution for preventing pH from changing suddenly by external environment. Phosphate buffer solution of pH 7.4 was used. Phosphate buffer solution is composition of potassium phosphate dibasic (K_2HPO_4) solution and potassium phosphate monobasic (KH_2PO_4). To get 0.2 M of dibasic solution, anhydrated form of potassium phosphate dibasic of 24.8 g was dissolved in deionized water and the total volume of solution was 1 liter. 0.2 M of monobasic required 13.9 g in 500 ml volume of solution. Then 57 ml of monobasic solution and 243 ml of dibasic solution were mixed to get pH 7.4 solution. In the mixture, 600 ml of deionized water was added [11]. In 50 ml of the phosphate buffer solution, 0.0165 g of potassium ferricyanide ($\text{K}_3[\text{Fe}(\text{CN})_6]$) and 0.0211 g of potassium ferrocyanide ($\text{K}_4[\text{Fe}(\text{CN})_6]$) were dissolved to get 1 mM of ferricyanide and ferrocyanide ($\text{Fe}(\text{CN})_6^{3-}/\text{Fe}(\text{CN})_6^{4-}$) solution. From the 1 mM of $\text{Fe}(\text{CN})_6^{3-}/\text{Fe}(\text{CN})_6^{4-}$ solution, 5 ml was taken off and add 45 ml of phosphate buffer solution to get 0.1 mM of $\text{Fe}(\text{CN})_6^{3-}/\text{Fe}(\text{CN})_6^{4-}$ solution. From the same ways, 10 μM and 2 μM of $\text{Fe}(\text{CN})_6^{3-}/\text{Fe}(\text{CN})_6^{4-}$ solution were obtained.

Counter electrode was integrated in the device as patterned gold and reference electrode was commercial product made by World Precision Instruments, Inc. Gold pattern was tested as a reference electrode as well. The integrated gold reference electrode had offset compared with a commercial one. The purpose of this study is relative comparison between a new structure and a planar electrode, so gold electrodes provided the same information. For convenience, all the experiments used gold reference electrodes.

2. Measurement Methods

The important principles of electroanalytical chemistry used in this paper are cyclic voltammetry and chronoamperometry. Voltammetry is based on the measurement of the current-voltage relationship in an electrochemical cell consisting of electrodes in a solution. A potential is applied to the sensor and a current proportional to the concentration of the electroactive species of interest is measured. A triangular potential waveform is applied to the electrochemical cell. The scan rate of a cyclic voltammetry (CV) can be varied typically over the range from 10 mV s⁻¹ to 100 mV s⁻¹. The measured current at the working electrode is the response of a cyclic voltammetry. A peak in the current is observed due to the combined effect of the decrease of the electrode surface concentration and the expansion of the diffusion layer with time. In the reverse scan a peak is also observed; this peak is due to the electrochemical reaction of intermediates or products of the reactions during the forward scan.

Amperometry is a special case of voltammetry where the potential is kept constant as a function of time, which is called chronoamperometry. The applied potentials for two working electrodes are kept constant at reduction and oxidation potential shown in voltammogram. Theoretically the current decreases as $t^{-0.5}$. In practical experiments, however, it is found that the current reaches a limiting value after approximately tens of second. The constant current as a function of time is related to the convection of the solution; after some time the thickness of the diffusion layer becomes constant as a function of time. The steady state current then recorded for different sample concentrations. For amperometric measurements, a linear relation of the current as a function of sample

concentration was also found. An important advantage of amperometry is that it is a fast technique [12].

There is another criterion to determine sensor performance, which is called detection limit. Blank signal was measured in order to calculate detection limit for each electrode. The minimum distinguishable analytical signal S_m is then taken as the sum of the mean blank signal \bar{S}_{bl} plus a multiple k of the standard deviation of the blank. In many cases, $k = 3$ [13]. That is,

$$S_m = \bar{S}_{bl} + kS_{bl} \dots\dots\dots (1)$$

The slope that was obtained in chronoamperometry was used to convert S_m to c_m , which is defined as the detection limit [14]. That is, the detection limit is given by

$$c_m = \frac{S_m - \bar{S}_{bl}}{m} \dots\dots\dots (2)$$

The above equations can be modified as follows for easy calculation;

$$c_m = \frac{kS_{bl}}{m} \dots\dots\dots (3)$$

In this case, blank signal was measured three times because of limited number of devices.

IV. RESULTS AND DISCUSSION

1. Results

Sensor tests were done by a planar electrode and an air bridge type electrode. The planar electrode had 50 μm gap and 40 μm width, and the air bridge type electrode also had 50 μm gap gap, 40 μm width, and 5 μm distance between upper and lower electrode. They had the same dimension for performance comparison. We used CHI832 (CH Instrument, USA) for electrochemical experiments.

Cyclic voltammetry of air bridge type electrode was drawn to find reduction and oxidation potential. Small drop of sample of which volume is about 10 μl was put on the working electrode. Thereafter, chronoamperometry was carried out with applying reduction potential on working electrode 1 and oxidation potential on working electrode 2. WE 1 and 2 connection may be swapped because they are symmetric. For a given concentration, the current was measured for 5 min. After measuring 2 μM , 10 μM , 100 μM , and 1 mM, the current-time and current-

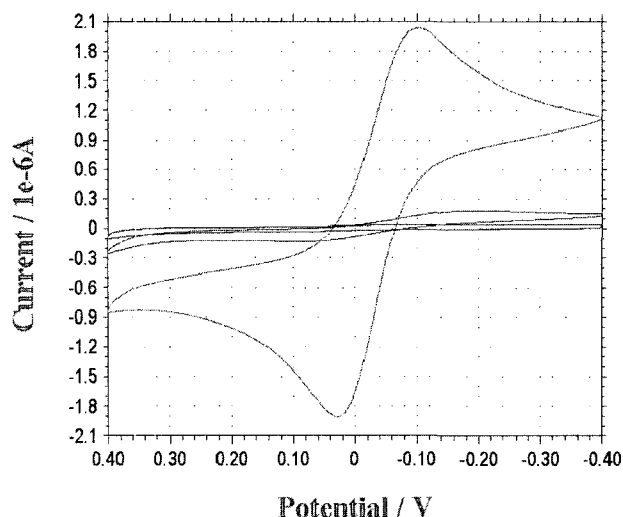


Fig. 7. Cyclic voltammety of the air bridge type electrode. Reduction potential peak is about -0.1 V and oxidation potential peak is about 0.05 V vs. gold reference electrode

concentration were plotted and the slope of current-concentration was calculated for comparison with planar type electrodes.

The result of cyclic voltammety of air bridge type electrode was drawn in Figure 7. The largest peak was made by 1 mM of $Fe(CN)_6^{3-}/Fe(CN)_6^{4-}$, the second by 100 μM , and the smallest by 10 μM , respectively. Voltammogram of 2 μM was omitted because the signal was too small to show peaks. Reduction potential was about -0.1 V and oxidation potential was about 50 mV.

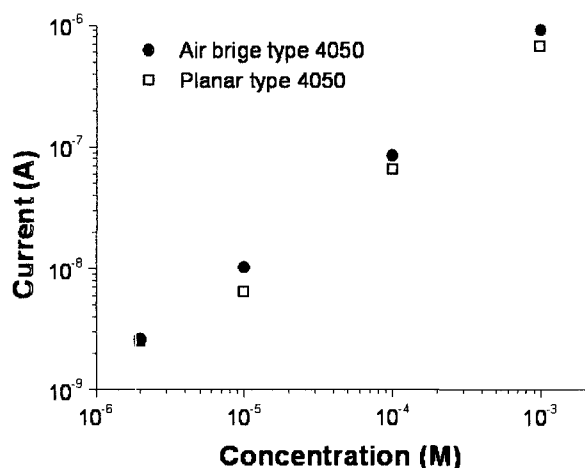


Fig. 8. Current and concentration relation of the air bridge type (round dots) electrode and planar IDA electrode (square dots). They have same finger gap, but the air bridge electrode showed better sensitivity because it has 5 μm electrode gap. The slope of air bridge type electrode was 9.1×10^{-4} and that of planar IDA electrode was 6.6×10^{-4} .

Applied potentials lower than reduction potential and higher than oxidation potential were -0.2 and 0.2 V for chronoamperometry. Keeping the given potential, samples were injected. Figure 8 shows the slope of current increment to concentration change by log scale. As stated in III.2 measurement methods, the relation between current and concentration is linear. The slope of the air bridge electrode was 9.1×10^{-4} and that of planar IDA electrode was 6.6×10^{-4} . The air bridge electrode showed better sensitivity because it has 5 μm electrode distance resulting in virtually reducing the finger gap to one tenth.

From the equations (1), (2) and (3), detection limit was calculated. The slope of air bridge type electrode was 9×10^{-4} , that is, $m = 9 \times 10^{-4}$ and $s_{bl} = 2.9 \times 10^{-10}$. Thus the detection limit was three times 2.9×10^{-10} divided by 9×10^{-4} , about 1 μM .

2. Discussion

Because the slope of current and concentration is proportional to analytical sensitivity, the air bridge type electrode has almost same sensitivity with the planar IDA electrode of which electrode gap is 20 μm although it has 50 μm finger gap. That was proven by cyclic voltammety and chronoamperometry among many electrochemical techniques. The detection limit is about 1 μM of the electrode. In conclusion, the thickness control method can replace nano-patterning for narrowing finger gap.

One of the problems of the fabrication is the surface smoothness of electroplating. The rough surface of copper resulted in rough gold. Because of the lack of uniformity, some parts of upper electrodes disappeared after gold etching. This problem can be avoided by long time sputtering of copper or aluminum. By sputtering, we can get uniform surface of sacrificial layer and tune the thickness much more precisely.

V. CONCLUSIONS

Copper was sputtered on gold patterned glass wafer for electroplating seed material. The copper electroplating condition is at Table 1. About 5 μm of copper was plated. Chrome and gold were sputtered on the copper. SU-8 2025

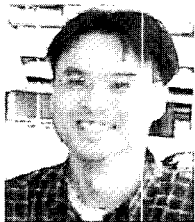
negative PR was patterned on the gold surface for protection. The SU-8 patterned wafer was soaked in gold etchant and chrome etchant consecutively until the copper sacrificial layer was disappeared. By the above fabrication, air bridge type electrodes were obtained. The distance was 5 μm , the finger gap was 40 μm and finger width was 50 μm . The completed electrode showed better sensitivity than the planar IDA electrode with the same dimension. The most powerful merit of the air bridge type is that the small electrode distance can be made by controlling the thickness of sacrificial layer between upper and lower electrode, which is much more economical. Theoretically the distance can be reduced to hundreds of nanometers. The difficult and expensive nano-patterning techniques can be replaced by thickness control of sacrificial layer in order to make electrodes with high sensitivity.

ACKNOWLEDGMENTS

This work was supported by a grant (04K1401-00411) from Center for Nanoscale Mechatronics & Manufacturing, one of 21st Century Frontier Research Programs, Ministry of Science and Technology, Korea. The authors are grateful for Digital Nanolocomotion Center, KAIST, Korea.

REFERENCES

- [1] S.K.Kim, J.H.Thomas, P.J.Hesketh, C.Li, B.H.Halsall, W.R.Heineman, "Comb Interdigitated Arrays (IDA) Electrodes for More Rapid and Sensitive Bead-based Immunoassay," *IEEE MEMS*, pp. 435-438, 2003.
- [2] R.Kurita, H.Tabei, Z.Liu, T.Horiuchi, and O.Niwa, "Fabrication and electrochemical properties of an interdigitated array electrode in a microfabricated wall-jet cell," *Sensors and Actuators*, Vol. B 71, pp. 82-89, 2000.
- [3] O.Niwa, Y.Xu, H.B.Halsall, and W.R.Heineman, "Small-Volume Voltammetric Detection of 4-Aminophenol with Interdigitated Array Electrodes and Its Application to Electrochemical Enzyme Immunoassay," *Anal. Chem.*, Vol. 65, pp. 1559-1563, 1993.
- [4] M.Morita, O.Niwa, and T.Horiuchi, "Interdigitated array microelectrodes as electrochemical sensors," *Electrochimica Acta*, Vol. 42, pp. 3177-3183, 1997.
- [5] O.Niwa, M.Morita, and H.Tabei, "Electrochemical Behavior of Reversible Redox Species at Interdigitated Array Electrodes with Different Geometries: Consideration of Redox Cycling and Collection Efficiency," *Anal. Chem.*, Vol. 62, pp. 447-452, 1990.
- [6] A.E.Cohen, R.R.Kunz, "Large-area interdigitated array microelectrodes for electrochemical sensing," *Sensors and Actuators*, Vol. B 62, pp. 23-29, 2000.
- [7] H.Schift, R.W.Jaszewski, C.David, and J.Gobrecht, "Nanostructuring of Polymers and Fabrication of Interdigitated Electrodes by Hot Embossing Lithography," *Microelectronic Engineering*, Vol. 46, pp. 121-124, 1999.
- [8] J.H.Thomas, S.K.Kim, P.J.Hesketh, H.B.Halsall, and W.R.Heineman, "Microbead-based electrochemical immunoassay with interdigitated array electrodes," *Analytical Biochemistry*, Vol. 328, pp. 113-122, 2004.
- [9] N.Honda, K.Emi, T.Katagiri, T.Irita, S.Shoji, H.Sato, T.Homma, T.Osaka, M.Saito, J.Mizuno, Y.Wada, "3-D Comb Electrodes for Amperometric Immuno Sensors," *IEEE Transducers*, pp. 1132-1135, 2003.
- [10] A.E.Olsen, "Bright Acid Sulfate Copper Plating," *AESF Illustrated lectures*, 1995.
- [11] http://cancer.rutgers.edu/stg_lab/protocols/Phosphate%20buffer.htm
- [12] M.Lambrechts and W.Sansen, *Biosensors; "Microelectrochemical Devices," IOP Publishing*, pp. 6-10, 82-93, 192-194, 1992.
- [13] G.L.Long and J.D.Winefordner, "Limits of Detection: Are They Real?" *Anal. Chem.*, Vol. 55, 712A, 1983.
- [14] Skoog, Holler, and Nieman, "Principles of Instrumental Analysis, 5th edition," *Harcourt College Publishers*, pp. 12-14, 1996.



Yuheon Yi He received the B.S. degree in electronic and electrical engineering from POSTECH (Pohang University of Science and Technology) in 1999 and M.S. degree in biosystems from Korea Advanced Institute of Science and Technology (KAIST) in 2004. He is currently working at the DongbuAnam Semiconductor Inc. His current research interests include bioMEMS, RF MEMS and lab-on-a-chip.



Je-Kyun Park He received the B.S. and M.S. degrees in food science and technology from Seoul National University in 1986 and 1988, respectively, and his PhD degree in biotechnology from Korea Advanced Institute of Science and Technology (KAIST) in 1992. From 1996 to 1997 he was a postdoctoral fellow in the Department of Biomedical Engineering at Johns Hopkins University, Baltimore, USA. From 1992 to 2002 he worked at the LG Electronics Institute of Technology, Seoul, Korea, where he was the group leader of the bioelectronics research. In 2002, he joined the Department of BioSystems at KAIST as an associate professor. His research interests are focused on nanobiotechnology and have included bioMEMS, bioelectronic devices and cell-based microsystems.